AMERICAN METEOROLOGICAL SOCIETY

Journal of Hydrometeorology

EARLY ONLINE RELEASE

The DOI for this manuscript is doi: 10.1175/JHM-D-15-0027.1

Rhee, J., and J. Cho, 2015: Future changes in drought characteristics: Regional analysis for South Korea under CMIP5 projections. J. Hydrometeor. doi:10.1175/JHM-D-15-0027.1, in press.

Future changes in drought characteristics: Regional analysis for South Korea under CMIP5 projections

Jinyoung Rhee* and Jaepil Cho

Climate Research Department, APEC Climate Center, Busan, 48058, Republic of Korea

* Corresponding author address: Jinyoung Rhee, APEC Climate Center, 12 Centum 7-ro, Haeundae-gu, Busan, 48058, Republic of Korea.

E-mail: jyrhee@apcc21.org

ABSTRACT

The future changes in drought characteristics were examined on a regional scale for South Korea, in northeastern Asia, using seventeen bias-corrected Coupled Model Intercomparison Project Phase 5 (CMIP5) projections of Representative Concentration Pathway (RCP) 4.5 and 8.5 scenarios. The frequency of severe or extreme drought, based on the Standardized Precipitation Index (SPI) and Standardized Precipitation-Evapotranspiration Index (SPEI) drought indices, with time scales of 1-, 3-, and 12-months, was considered as well as the average duration based on SPEI1. A Multi-Model Ensemble (MME) was produced using selected models, and future changes were investigated in terms of both drought frequency and the average duration for the entire area and four river basins. The changes in drought frequency largely depend on the selection of a drought index, rather than climate projection scenarios. SPEI3 mostly projected future increases in drought frequency, while SPI3 showed varied projections. SPI12 projected decreases in drought frequency for both scenarios in the

study area, while differences between river basins were observed for SPEI12. Increases in the average duration of droughts were projected based on SPEI1, indicating an increase in persistent short-term droughts in the future. The results emphasize the importance of regional and sub-regional scale analysis in northeastern Asia. The findings of the study provide valuable information that can be used for drought-related decision making, which could not be obtained from studies on a global spatial scale.

1 Introduction

Drought can have a tremendous impact on society and ecosystems. There are several categories of droughts, including meteorological, soil moisture (or agricultural), hydrological, and socioeconomic drought. The definition of drought is well documented in the Special Report on Managing the Risks of Extreme Events and Disasters to Advance Climate Change Adaptation (SREX). Meteorological drought is caused by a lack of precipitation; soil moisture drought is related to a deficit of soil moisture; and hydrological drought is caused by abnormally low streamflow (IPCC 2012). Socioeconomic drought occurs as the result of interactions of non-climatic factors, such as human water use and climatic influences.

Although the main cause of drought is a deficit of precipitation, other factors such as temperature, wind speed, and soil moisture are strongly involved in the occurrence of drought, and large uncertainties still exist with regard to the land–atmosphere feedback related to drought (Seneviratne et al. 2012). While many variables are important in the processes related to drought, observations are seldom available. A variety of drought indices based on standardized anomalies of climate variables are generally used to monitor and assess drought conditions. Future drought outlook may also be possible based on drought indicators with climate change projections. To properly monitor and assess the current status or to project future droughts, the selection of drought indices for each type of drought of interest is undoubtedly important. The use of different drought indices may produce dissimilar projections of future drought occurrence, thus appropriate drought indices, which are locally applicable, should be used for impact assessments especially for regional studies (Burke and Brown 2008). Recent studies of future drought projections based on the third phase of the Coupled Model Intercomparison Project (CMIP3) are well summarized by Seneviratne et al.

(2012). Outputs from the coupled ocean-atmosphere general circulation models are archived in the CMIP3 multi-model dataset, based on the Intergovernmental Panel on Climate Change (IPCC) Fourth Assessment Report (Meehl et al. 2007). Orlowsky and Seneviratne (2013) also analyzed future drought trends using CMIP5 projections based on indices for meteorological and soil moisture drought. The fifth phase of the CMIP includes recent climate model experiments from the IPCC Fifth Assessment Report (Taylor et al. 2012a). These studies were performed on a global scale and provide information on the projected change in drought occurrence with accompanying uncertainties. However, global scale analysis may not deliver sufficient information on local and regional changes, due to its coarse spatial resolution. Orlowsky and Seneviratne (2013) projected no increased drought occurrence in the East Asia region based on consecutive dry days (CDD) and soil moisture anomalies (SMA), while there are contrasting results from regional studies (*e.g.*, Kim et al. 2014, and Kwak et al. 2015). Regional analysis of future drought projection is essential for impact and vulnerability studies, as well as for appropriate climate change adaptation.

Future changes in drought occurrence were investigated in this study, with a detailed analysis for South Korea in northeastern Asia. The aims of the study were: (1) to compare future changes of drought characteristics based on different drought indicators as well as different climate change scenarios, and (2) to examine the importance of regional-scale analysis in northeastern Asia. The effect of a deficit of precipitation was examined using the 1-, 3-, and 12-month Standardized Precipitation Index (SPI1, SPI3, and SPI12); the additional influence of an increased evaporative demand was considered using the 1-, 3-, and 12-month Standardized Precipitation-Evapotranspiration Index (SPEI1, SPEI3, and SPEI12). Because substantial warming is projected due to climate change (IPCC, 2012) and SPEI has the ability

to account for both temperature and precipitation, it can identify the changes in drought characteristics associated with changes in evaporative demand (Vicente et al. 2010).

Historical droughts in South Korea have both short and long time scales. Spring drought is relatively short (<200 days), because the summer rainy season follows immediately after. In contrast, summer drought is long (>200 days), because it tends to be dry throughout autumn and winter (Kim et al. 2011). However, serious drought events have also been frequently observed in the study area, due to a lack of precipitation for <90 days (Yoo et al. 2013). Short- and long-term droughts were examined on a 3- and 12-month time scale, respectively (WMO, 2012). The frequency of severe or extreme drought was investigated, as well as the average duration of drought based on a 1-month time scale.

The analyses were performed based on bias-corrected CMIP5 simulations of the Representative Concentration Pathway (RCP) 4.5 and 8.5 scenarios from 1976 to 2100. The use of combined results from several models, such as a multi-model mean, generally improves the forecast proficiency and reliability of individual models (Tebaldi and Knutti 2007; Gillett et al. 2002, Lambert and Boer 2001). Seventeen different Global Climate Models (GCMs) were individually examined, in addition to their Multi-Model Ensemble (MME), to observe changes in drought characteristics. For a detailed analysis, four major river basins were also examined individually, in addition to an analysis of the entire area (ENT).

2 Data and Methodology

2.1 Study Area and Observation Data

96 The study was performed in South Korea, in northeastern Asia (Figure 1). There are
97 four major river basins in the southern part of the peninsula: the Han, Nakdong, Geum, and
98 Yeongsan-Sumjin river basins. The locations and number of Automated Synoptic Observing
99 System (ASOS) weather stations in the river basins are shown in Table 1. Monthly
100 precipitation, and maximum and minimum temperature data were obtained from the Korea
101 Meteorological Administration (KMA); only weather stations with no missing monthly data
102 for 1976–2005 were used in the study.

103 Based on the Köppen–Geiger climate classification system, the study area has a
104 humid continental climate in the northern part and a humid subtropical climate in the
105 southern part and eastern coastal region. Annual average precipitation is about 1,200–1,500
106 mm in the northern part and 1,000–1,800 mm in the southern areas. The area is affected by
107 the East Asian Monsoon. Boreal summer precipitation is dominant and occupies about 50–60%
108 of the total precipitation. Annual average temperature is around 10–15°C (KMA 2011).

109 With more than three quarters of the land being mountainous, the topography is one
110 of the main factors affecting the climate of the area (MLIT 2013). Agricultural land areas are
111 largely located in the western part of the country; rice paddies that provide the staple diet of
112 the region are concentrated in the Geum River Basin. Irrigation systems are widely used,
113 enabling a sufficient water supply for industrial and municipal use. However, there are still
114 some areas with no irrigation, such as the highland regions; these regions are affected
115 significantly by drought, even over the short term. Spring droughts are the most challenging
116 issue in the study area due to the effect on rice production, while winter droughts mainly
117 affect fruit growth.

118

119 *2.2 CMIP5 Projections*

120 The RCP4.5 (a stabilization scenario, in which the total radiative forcing stabilizes to
121 4.5 W/m shortly after 2100) and RCP8.5 (characterized by increasing greenhouse gas
122 emissions over time leading to a radiative forcing of 8.5 W/m in 2100) scenarios for the
123 IPCC Fifth Assessment Report were used in this study. Seventeen global climate models
124 (GCMs) were selected to provide data for precipitation, and maximum and minimum
125 temperature from 1976 (Table 2); their daily data for historical (1976–2005) and future
126 (2006–2100) periods were obtained from the Earth System Grid Federation
127 (http://pcmdi9.llnl.gov/esgf-web-fe/).

128 Daily data for the entire period (1976–2100) were aggregated to monthly values,
129 downscaled, and bias-corrected using a non-parametric quantile mapping method against the
130 observation data from 58 ASOS weather stations. The non-parametric approach is known to
131 be better than the parametric approach for correcting system biases, because it uses the actual
132 distribution of the observed and simulated data, without estimating a probability distribution
133 function (Gudmundsson et al. 2012). Quantile-based mapping methods have been widely
134 used to downscale and correct Regional Climate Models (RCMs) (*e.g.*, Ashfaq et al. 2010;
135 Themeßl et al. 2012; Sunyer et al., 2012) as well as GCMs (*e.g.*, Wood et al., 2004; Ines and
136 Hansen, 2006; Bo´e et al., 2007; Li et al., 2010). Although it removes biases in GCM
137 simulations efficiently and overcomes scale mismatches, it is doubtful that the corrected
138 simulation data would be able to represent real changes (Eden et al. 2012). However, in this
139 study, this concern was not considered, because the comparisons were performed using the

140 drought characteristics of frequency and average duration. Differences between the
141 observation and simulation data for each quantile were calculated and used for the bias-
142 correction of the future period.

143

144 *2.3 Drought Indices*

145 There are many sources of uncertainty in the future projection of drought. Taylor et al.
146 (2012b) examined four sources of uncertainty: climate model uncertainty, future scenario
147 uncertainty, drought index uncertainty, and drought threshold uncertainty. They found that the
148 selection of the drought index is the most important factor affecting the uncertainty in future
149 drought projections (Taylor et al. 2012b). This indicates that the choice of drought index may
150 affect the results of drought impact assessment. Burke and Brown (2008) used four different
151 drought indices to assess the uncertainty in future drought projections: the SPI, the
152 precipitation and potential evapotranspiration anomaly (PPEA), the Palmer drought severity
153 index (PDSI), and the soil moisture anomaly (SMA). In their study, only the SPI projected
154 little change in the land surface areas under drought, while the other three indices projected
155 otherwise. This is because the SPI is based only on precipitation, while the other indices
156 include measurements of the atmospheric moisture demand (Burke and Brown 2008).

157 In this study, both the SPI and SPEI were considered for the analyses. SPI (McKee et
158 al. 1993) is the recommended index for universal meteorological drought by the World
159 Meteorological Organization (Hayes et al. 2011). A long time series of precipitation data were
160 obtained, and aggregated into a desired time scale, fitted to a certain probability distribution,
161 and then standardized by being converted to a normal distribution (Guttman 1999). The

parameters for fitting data to a probability distribution, such as gamma or Pearson Type-III, are determined based on a selected calibration period. Lee and Kim (2012) performed goodness-of-fit tests for 15 different probability distributions for the calculation of SPI in South Korea, including the gamma, general extreme value, Gumbel, log-Gumbel, log-normal, log-Pearson type-III, normal, Pearson type-III, Weibull, and Wakeby distributions and found that the log-Gumbel, gamma, general extreme value, Gumbel, log-normal, and Weibull distribution types were appropriate. In this study, the gamma distribution was used for SPI1, SPI3, and SPI12. Because SPI is based only on precipitation, it can be easily obtained for weather stations or regions with limited data for other variables. However, it has been noted that the SPI cannot consider the effect of other variables, such as temperature, by assuming their stationarity (Vicente-Serrano et al. 2010).

SPEI uses potential evapotranspiration as well as precipitation as a measure for atmospheric moisture demand (Vicente-Serrano et al. 2010). Although it is sometimes demanding to archive data for variables other than precipitation, it is possible for SPEI to account for the plausible effects of temperature variability in a changing climate (Vicente-Serrano et al. 2010). Potential evapotranspiration as an input variable for SPEI was calculated using the Hargreaves method based on the maximum and minimum temperature (Hargreaves et al. 1985). The Penman–Monteith method is known to be the most robust (Begueria et al. 2014), but the Hargreaves method requires fewer variables and enabled a large number of GCMs to be used in this study. A long time series of the difference between precipitation and potential evapotranspiration was obtained, aggregated into the desired time scale, fitted to the log-logistic probability distribution, and then standardized. Vicente-Serrano et al. (2010) performed goodness-of-fit tests for several different distributions for the calculation of SPEI,

185 including the Pearson type-III, log-normal, general extreme value, and log-logistic
186 distributions; all were appropriate for the 11 observatories located in different regions of the
187 world. Sohn et al. (2013) also used the log-logistic probability distribution to calculate SPEI
188 in a winter-to-spring drought study in South Korea. In this study, the log-logistic distribution
189 was used for SPEI1, SPEI3, and SPEI12.

190 The calibration period of 1976–2005 was used for all drought indices. Only severe or
191 extreme drought (drought index value ≤ -1.50) was considered (Table 3).

192

193 *2.4 Frequency of Drought*

194 Drought frequency was defined as the number of months suffering severe or extreme
195 drought among all months during a 30-year period. For each drought index and model, the
196 frequencies were calculated for both historical and future periods. There were 66 of 30-year
197 periods during 2006–2100, starting with the 30-year period 2006–2035 (a period ending in
198 2035; PEY2035) and ending with the 30-year period 2071–2100 (a period ending in 2100;
199 PEY2100).

200 The calculated frequencies from individual models were compared to the values
201 based on observation data for the historical period using Dunnett multiple comparisons, to
202 evaluate the performance of CMIP5 simulations and the bias correction methodology.
203 Dunnett's multiple comparisons provide comparison results between multiple treatment
204 groups, with a single control group (Dunnett, 1955), and is widely used in association with a
205 one-way analysis of variance (ANOVA). The null hypothesis (H0) is that there is no
206 difference between means; a significance level of 0.05 ($\alpha = 0.05$) was used. Model simulation

results that do not reject H0 were considered to be "consistent" with the observation data in this study. The MME of frequencies based on simple averaging with equal weights were calculated using all 17 models (MME_all), in addition to using selected models that did not reject H0 for the historical period (MME_part).

The frequencies from individual models, MME_part, and MME_all for the future period (PEY2035–PEY2100) were compared to the values for the historical period, also using Dunnett multiple comparisons, to determine future changes in drought frequency.

2.5 Average Duration of Drought

An additional variable, the average duration of drought, was defined as the total number of individual months with severe or extreme drought divided by the number of drought events (which considers consecutive drought months as one drought event) for a 30-year period (Eq. (1)). For example, if the number of months with severe or extreme drought is 52, and the number of drought events is 36 during the 30-year period of 2006–2035, the average duration becomes 52 / 36 = 1.44. Large values generally indicate the existence of persistent short-term drought events (with a longer run length), while small values indicate the frequent, but intermittent occurrence, of short drought events.

$$\text{Average Duration} = \frac{number\ of\ individual\ months\ with\ Severe\ or\ Extreme\ drought}{number\ of\ drought\ events} \quad \text{(Eq. 1)}$$

Average duration of drought was only calculated for SPI1 and SPEI1. The average durations from individual models, MME_part, and MME_all for the historical period (1976–2005) were calculated and compared to the values based on the observation data using

228 Dunnett multiple comparisons. The values for the future period (PEY2035–PEY2100) were
229 also calculated and compared to the values for the historical period, also using Dunnett
230 multiple comparisons, to determine future changes in the average duration of drought.

231 The average duration of drought for SPI1 and SPEI1 was used in this study in
232 addition to exploring the 3- and 12-month SPI and SPEI to determine if it can provide
233 additional information on the future changes of drought characteristics. If two months are
234 interspersed by one month experiencing severe or extreme drought, the three-month period
235 may or may not appear as one drought event with a 3-month time scale, while the period is
236 separated into two individual drought events with a 1-month time scale. Because short-term
237 drought may pose a serious threat to agriculture, based on past experiences in the study area,
238 its detection is very important.

239

240 **3 Results and Discussion**

241 *3.1 Frequency of Drought*

242 *Historical Period*

243 The frequencies of severe or extreme droughts based on 17 individual models,
244 MME_all, and MME_part during the historical period 1976–2005 were compared to
245 observation data using Dunnett multiple comparisons for 58 ASOS stations. Model
246 performance varied by drought index and by river basin (Figure 2). All 17 models rejected the
247 H0 and produced larger means than the observation data for SPI1 for the ENT and all river
248 basins (RIV1-4), and for SPI3 for the Han River Basin (RIV1). This was likely due to the

large uncertainty in the projected precipitation for the weather stations belonging to each basin. The uncertainty was smaller for SPI12, with a longer time scale, and for SPEI3 and SPEI12 where the temperature term is included. For SPEI1, SPI12, and SPEI12, some models produced larger means, while others produced smaller means than the observation data (Figure 2). The behavior was similar between models for SPI3 and SPEI3. Many models produced larger means than the observation data for SPI3, while many had smaller means than the observation data for SPEI3.

The MME_all was affected by the models that rejected the H0, and also rejected the H0 for some drought indices and regions. This indicates that MME_all could not produce consistent frequencies of drought with the observation data. Because MME_part was based on only the models where the H0 was not rejected, it produced results that were consistent with the observation data.

Future Period

The future changes of severe or extreme drought frequencies were examined for each drought index, climate change scenario, and river basin, using Dunnett multiple comparisons for each future period (Figures 3–8). The H0 for a 30-year period among PEY2035–PEY2100 is that there is no difference in drought frequency between the historical period and the selected period. Larger and smaller means compared to the historical period indicate a projected increase and decrease in the frequency of severe or extreme drought in the future, respectively.

The analysis was first performed using MME_part for all 58 weather stations, to

examine the range of drought frequencies from weather stations in the ENT and each river basin (Figures 3–6). The boxplots show the distribution of drought frequencies for the weather stations located in the corresponding river basin. Because there was no individual model consistent with the observation data during the historical period for SPI1 in the ENT and all river basins, and for SPI3 for the Han River Basin, the analysis was not performed for these cases.

No significant future change was expected based on RCP4.5 in the ENT, while RCP8.5 projected some periods with increased and decreased drought frequency based on SPI3 (Figure 3a). Results in other river basins varied. RCP4.5 and RCP8.5 in the Nakdong River Basin (Figure 3b) and RCP4.5 in the Yeongsan-Sumjin River Basin (Figure 3d) projected decreases in drought frequency based on SPI3, while increases were expected based on RCP8.5 in the Geum River Basin (Figure 3c). Decreases in drought frequency were projected for most future periods based on SPI12 for the entire area and all river basins, and for both RCP4.5 and RCP8.5 (Figure 4).

For SPEI1, the H0 was rejected for all future periods for both RCP4.5 and RCP8.5 in the ENT as well as all river basins, and increases in drought frequency were projected (data not shown). SPEI3 produced similar results to those for SPEI1, with the H0 not rejected in only the early future periods in the Geum and Yeongsan-Sumjin River Basins (Figure 5). Differences between river basins were observed for SPEI12 (Figure 6). In the Nakdong and Geum River Basins, increases in drought frequency were projected in the later future periods based on RCP8.5 (Figures 6c,d), while in the Han River Basin decreases in drought frequency were only projected in the later future periods based on RCP4.5 (Figure 6b).

293 The analysis was also performed using the individual models used for MME_part
294 and station-averaged frequencies, to examine the range of drought frequencies between
295 individual models in the ENT and all river basins (Figures 7 and 8). The boxplots show the
296 distribution of drought frequencies for individual models. As observed in the results with
297 MME_part, large differences were apparent between the river basins for SPI3 and SPEI12.
298 Averaging the drought frequencies for weather stations can cancel out the projected increases
299 and decreases of drought frequency. Station-averaged drought frequencies for SPI3 and
300 SPEI12 for all future periods did not reject the H0 for the ENT and all river basins, and for
301 both RCP4.5 and RCP8.5 (data not shown).

302 For SPI12, decreases in drought frequency were projected for both RCP4.5 and
303 RCP8.5 during the later future periods for the ENT (Figure 7a) and the Geum River Basin
304 (Figure 7d), only for RCP4.5 in the Yeongsan-Sumjin River Basin (Figure 7e), and only for
305 RCP8.5 in the Han River Basin (Figure 7b).

306 Similar to the results based on MME_part, increases in drought frequency were
307 expected for most future periods for SPEI1 for both RCP4.5 and RCP8.5, and for the ENT
308 and all river basins (data not shown). Differences between river basins were apparent for
309 SPEI3. Increases in drought frequency in the later future periods were projected for both
310 RCP4.5 and RCP8.5 only in the Nakdong River Basin (Figure 8c), and for RCP8.5 in the Han
311 and Yeongsan-Sumjin River basins (Figures 8b,e).

312 The lengths of future periods with projected increases or decreases in drought
313 frequency were much shorter when station-averaged data and individual models were used
314 compared with when individual station data and MME_part were used. As discussed earlier,

315 this was because the differences between weather stations were flattened due to averaging.

316

317 *3.2 Average Duration of Drought*

318 As with the frequency of drought, the future changes in the average duration of
319 severe or extreme drought were examined for each climate change scenario and river basin
320 using Dunnett multiple comparisons for each future period (Figures 9 and 10). The H0 for a
321 30-year period among PEY2035–PEY2100 is that there is no difference in average duration
322 between the historical period and the selected period. Larger and smaller means compared to
323 the historical period indicate a projected increase and decrease in the average duration of
324 severe or extreme drought in the future, respectively. The analysis was performed only for
325 SPEI1, because MME_part could not be obtained for SPI1 as explained earlier.

326 The MME_part for all 58 weather stations were examined first, and then individual
327 models for MME_part and station-averaged average durations were used for analyses. The
328 average duration of drought was expected to increase compared with the historical period
329 based on both RCP4.5 and RCP8.5 during most future periods when MME_part and
330 individual weather station data were used (Figure 9), and during later future periods when
331 individual models for MME_part and station-averaged data were used (Figure 10).

332 Large average duration values indicate the occurrence of persistent short-term
333 drought events, while small values indicate the frequent but intermittent occurrence of short
334 drought events. Model simulations based on SPEI1 projected an increase in persistent short-
335 term droughts in the future compared with the historical period, especially toward the twenty-
336 second century. This may indicate an increase in the time scale of droughts in the study area

337 in the future.

338

339 **4 Conclusions**

340 The future changes of drought characteristics were examined on a regional spatial
341 scale over South Korea using 17 bias-corrected GCM model projections. The frequency of
342 severe or extreme drought based on the SPI and SPEI drought indices with time scales of 1-,
343 3-, and 12-months during the historical period from 1976–2005 were compared to the
344 quantities based on observation data. Appropriate models showing a consistency between
345 model simulation results and observation data were identified, and their MME was produced.
346 Future changes were then investigated to determine both the drought frequency and average
347 duration for the entire area and all river basins using the historical period as the calibration
348 period.

349 The differences between climate change scenarios were not obvious from the results.
350 This is because a trend analysis was not included in the study; only the changes in drought
351 characteristics in the future were examined through a comparison with the historical period.
352 Future increasing or decreasing trends were visually inspected, and no obvious difference
353 was observed between scenarios. There were some differences observed for SPI3 and SPEI12;
354 for example, RCP8.5 projected more increases in drought frequency than RCP4.5 for SPEI12
355 and for most river basins.

356 The projected future changes in drought frequency differed tremendously by drought
357 index. Most contrast was observed between SPEI3 and SPI12. While the results for both SPI3
358 and SPEI12 were somewhat mixed in the future period, with either increases or decreases in

drought frequency expected, SPEI3 mostly projected an increase in drought frequency, and SPI12 projected a decrease in drought frequency. The different results between SPI and SPEI were due to the variables used for each index, with SPI only using precipitation and SPEI using evaporative demand. Based on SPI, decreases in drought frequency were expected, especially in the long-term; whereas for SPEI, increases in drought frequency were projected, especially in the short-term. The importance of the selection of a drought index, as discussed by Taylor et al. (2012b) and Burke and Brown (2008), was emphasized again in this study.

The contrasting results for the future changes of drought characteristics also imply the importance of regional scale analysis in northeastern Asia. Sub-regional analysis may even be required. When station-averaged values for individual models for MME_part were used, the averaging frequencies or average durations for weather stations cancelled out the projected future increases and decreases of the drought characteristics. Although little differences between river basins were observed for drought frequencies based on SPEI3 and SPI12, and for average durations of drought based on SPEI1, some differences were still observed for drought frequencies based on SPI3 and SPEI12.

The average duration of drought was used in the study to examine changes in the persistence of short-term drought events, because even short-term droughts may be devastating in the study area. SPEI1 projected more persistent short-term drought events in the future, which also means an increase in the time scale of drought in the study area in the future.

The outcomes of this study provide valuable information that can be used for drought-related decision making of the study area, which could not be obtained from studies

on a global spatial scale. A global scale analysis may not deliver sufficient information on local and regional changes due to the coarse spatial resolution. A regional analysis of future drought projection is therefore essential for impact and vulnerability studies, and eventually for appropriate climate change adaptation.

There were some weaknesses in the study. Large-scale circulations inducing droughts were not considered; only precipitation and temperature variables at weather stations were bias-corrected to obtain drought index values. The use of advanced downscaling techniques, including changes in large-scale variables, will be examined in future studies.

Acknowledgement

This research was supported by the APEC Climate Center. The authors acknowledge the World Climate Research Programme's Working Group on Coupled Modelling, which is responsible for CMIP, and thank the climate modelling groups (listed in Table 2 of this paper) for producing and making available their model output.

References

Ashfaq, M., L. C. Bowling, K. Cherkauer, J. S. Pal, and N. S. Diffenbaugh, 2010: Influence of climate model biases and daily-scale temperature and precipitation events on hydrological impacts assessment: A case study of the United States. *J. Geophys. Res.*, **115**, D14116, doi:10.1029/2009JD012965.

Begueria, S., S. M. Vicente-Serrano, F. Reig, and B. Latorre, 2014: Standardized precipitation

402 evapotranspiration index (SPEI) revisited: parameter fitting, evapotranspiration models,
403 tools, datasets and drought monitoring. *Int*. *J*. *Climatol*., **34**, 3001-3023, doi:
404 10.1002/joc.3887.

405 Bo´e, J., L. Terray, F. Habets, and E. Martin, 2007: Statistical and dynamical downscaling of
406 the Seine basin climate for hydro-meteorological studies, *Int*. *J*. *Climatol*., **27,** 1643–
407 1655, doi:10.1002/joc.1602.

408 Burke, E. J., and S. J. Brown, 2008: Evaluating uncertainties in the projection of future
409 drought. *J*. *Hydrometeor.,* **9,** 292-299, doi: 10.1175/2007JHM929.1.

410 Dunnett, C. W., 1955: A multiple comparison procedure for comparing several treatments
411 with a control. *J*. *Am*. *Stat*. *Assoc*., **50,** 1096-1121, doi:
412 10.1080/01621459.1955.10501294.

413 Eden, J. M., M. Widmann, D. Grawe, and S. Rast, 2012: Skill, correction, and downscaling of
414 GCM-simulated precipitation. *J*. *Climate*, **25**, 3970-3984, doi: 10.1175/JCLI-D-11-
415 00254.1.

416 Gillett, N. P., F. W. Zwiers, A. J. Weaver, G. C. Hegerl, M. R. Allen, and P. A. Stott, 2002:
417 Detecting anthropogenic influence with a multi-model ensemble. *Geophys*. *Res*. *Lett*., **29**,
418 1970, doi: 10.1029/2002GL015836.

419 Gudmundsson, L., J. B. Bremnes, J. E. Haugen, and T. Engen Skaugen, 2012: Technical Note:
420 Downscaling RCM Precipitation to the Station Scale Using Quantile Mapping–a
421 Comparison of Methods. *Hydrol*. *Earth Syst*. *Sc*. *Discuss*., **9,** 6185–6201, doi:
422 10.5194/hessd-9-6185-2012.

423 Guttman, N. B., 1999: Accepting the Standardized Precipitation Index: A calculation
424 algorithm. *J. Amer. Water Resources Assoc.*, **35**, 311-322, doi: 10.1111/j.1752-
425 1688.1999.tb03592.x.

426 Hargreaves, G. L., G. H. Hargreaves, and J. P. Riley, 1985: Agricultural benefits for Senegal
427 River basin. *J. Irrig. Drain. Eng.*, **111**, 113-124, doi: 10.1061/(ASCE)0733-
428 9437(1985)111:2(113).

429 Hayes, M., M. Svoboda, N. Wall, and M. Widhalm, 2011: The Lincoln Declaration on
430 drought indices: Universal meteorological drought index recommended. *Bull. Amer.*
431 *Meteor. Soc.*, **92**, 485-488, doi: 10.1175/2010BAMS3103.1.

432 Ines, A. V., and J. W. Hansen, 2006: Bias correction of daily GCM rainfall for crop simulation
433 studies. *Agr. Forest Meteorol.*, **138**, 44–53, doi:10.1016/j.agrformet.2006.03.009.

434 IPCC (Intergovernmental Panel on Climate Change), 2012: *A Special Report of Working*
435 *Group I and II of the Intergovernmental Panel on Climate Change (IPCC)*. Cambridge
436 University Press. 594 pp.

437 Kim, D.-W., H.-R. Byun, K.-S. Choi, and S.-B. Oh, 2011: A spatiotemporal analysis of
438 historical droughts in Korea. *J. Appl. Meteor. Climatol.*, **50**, 1895-1912, doi:
439 10.1175/2011JAMC2664.1.

440 Kim, B. S., I. H. Park, and S. R. Ha, 2014: Future projection of droughts over South Korea
441 using Representative Concentration Pathways (RCPs). *Terr. Atmos. Occean. Sci.*, **25**,
442 673-688, doi: 10.3319/TAO.2014.03.13.01(Hy).

443 KMA (Korea Meteorological Administration), 2011: Climatological normal of Korea (1981-

2010). Publication number 11-1360000-000077-14. Seoul, Republic of Korea.

Kwak, J., S. Kim, V. P. Singh, H. S. Kim, D. Kim, S. Hong, and K. Lee, 2015: Impact of climate change on hydrological droughts in the upper Namhan River basin, Korea. *KSCE J. Civ. Eng.*, **19**, 376-384, doi: 10.1007/s12205-015-0446-5.

Lambert, S. J., and G. J. Boer, 2001: CMIP1 evaluation and intercomparison of coupled climate models. *Clim. Dynam.*, **17**, 83-106, doi: 10.1007/PL00013736.

Lee, J. H., and C. J. Kim, 2012: A multimodel assessment of the climate change effect on the drought severity-duration-frequency relationship. *Hydrol. Process.*, doi: 10.1002/hyp.9390.

Li, H., J. Sheffield, and E. F. Wood, 2010: Bias correction of monthly precipitation and temperature fields from Intergovernmental Panel on Climate Change AR4 models using equidistant 15 quantile matching, *J. Geophys. Res.*, **115**, D10101, doi:10.1029/2009JD012882.

McKee, T. B., N. J. Doesken, and J. Kleist, 1993: The relationship of drought frequency and duration of time scales. *Eighth Conf. on Appl. Clim.*, Amer. Meteor. Soc., Jan 17-23, 1993, Anaheim CA, 179-186.

Meehl, G. A., C. Covey, K. E. Taylor, T. Delworth, R. J. Stouffer, M. Latif, B. McAvaney, and J. F. B. Mitchell, 2007: The WCRP CMIP3 multimodel dataset: A new era in climate change research. *Bull. Amer. Meteor. Soc.*, **88**, 1383-1394, doi: 10.1175/BAMS-88-9-1383.

MLIT (Ministry of Land, Infrastructure, and Transport), 2013: 2013 Annual report on land

465 planning and use. 773 pp. (In Korean).

466 Orlowsky, B., and S. I. Seneviratne, 2013: Elusive drought: uncertainty in observed trends
467 and short- and long-term CMIP5 projections. *Hydrol*. *Earth Syst*. *Sc*., **17**, 1765-1781, doi:
468 10.5194/hess-17-1765-2013.

469 Seneviratne S. I. and Coauthors, 2012: Changes in climate extremes and their impacts on the
470 natural physical environment. *Managing the Risks of Extreme Events and Disasters to*
471 *Advanced Climate Change Adaptation*, C. B. Field, V. Barros, T. F. Stocker, D. Qin, D. J.
472 Dokken, K. L. Ebi, M. D. Mastrandrea, K. J. Mach, G.-K. Plattner, S. K. Allen, M.
473 Tignor, and P. M. Midgley, Ed., A Special Report of Working Group I and II of the
474 Intergovernmental Panel on Climate Change (IPCC). Cambridge University Press, 109-
475 230.

476 Sohn S.-J., J.-B. Ahn, and C.-Y. Tam, 2013: Six month-lead downscaling prediction of winter
477 to spring drought in South Korea based on a multimodel ensemble. *Geophys*. *Res*. *Lett*.,
478 **40**, 579-583, doi: 10.1002/grl.50133.

479 Sunyer, M., H. Madsen, and P. Ang, 2012: A comparison of different regional climate models
480 and statistical downscaling methods for extreme rainfall estimation under climate
481 change. *Atmos*. *Res*., **103**, 119-128, doi:10.1016/j.atmosres.2011.06.011.

482 Taylor, K. E., R. J. Stouffer, and G. A. Meehl, 2012a: An overview of CMIP5 and the
483 experiment design. *Bull*. *Amer. Meteor. Soc*., **93**, 485-498, doi: 10.1175/BAMS-D-11-
484 00094.1.

485 Taylor, I. H., E. Burke, L. McColl, P. Falloon, G. R. Harris, and D. McNeall, 2012b:

Contributions to uncertainty in projections of future drought under climate change scenarios. *Hydrol. Earth Syst. Sc. Discuss.*, **9**, 12613-12653, doi: 10.5194/hessd-9-12613-2012.

Tebaldi, C., and R. Knutti, 2007: Review: The use of the multi-model ensemble in probabilistic climate projections. *Phil. Trans. R. Soc. A.*, doi: 10.1098/rsta.2007.2076.

Themeßl, M. J., A. Gobiet, and G. Heinrich, 2012: Empirical-statistical downscaling and error correction of regional climate models and its impact on the climate change signal. *Climate Change*, **112**, 449–468, doi:10.1007/s10584-011-0224-4.

Yoo, J. Y., H. Song, T.-W. Kim, and J.-H. Ahn, 2013: Evaluation of short-term drought using daily Standardized Precipitation Index and ROC analysis. *J. Korean Soc. Eng.*, **33**, 1851-1860, doi: 10.12652/Ksce.2013.33.5.1851. (In Korean with English abstract).

Vicente-Serrano, S.M., S. Beguería, J. I. López-Moreno, 2010: A multiscalar drought index sensitive to global warming: The Standardized Precipitation Evapotranspiration. *J. Climate*, **23**: 1696-1718, doi: 10.1175/2009JCLI2909.1.

WMO (World Meteorological Organization), 2012: *Standardized Precipitation Index User Guide* (M. Svoboda, M. Hayes and D. Wood), (WMO-No. 1090). Geneva. 24 pp.

Wood, A. W., L. R. Leung, V. Sridhar, and D. P. Lettenmaier, 2004: Hydrologic implications of dynamical and statistical approaches to downscaling climate model outputs. *Climate Change*, **62**, 189-216, doi:10.1023/B:CLIM.0000013685.99609.9e.

506 **TABLES**

507

508 Table 1. Study area and the four major river basins in South Korea.

River Basin	Name	Area (km2)	Number of ASOS stations
ENT	Entire Area	99,133	58
RIV1	Han	32,200	15
RIV2	Nakdong	32,280	20
RIV3	Geum	17,767	13
RIV4	Yeongsan-Sumjin	16,886	10

509 Source: Water Information System, http://water.nier.go.kr/front/waterInfo/watershed01.jsp

510

511

512 Table 2. Characteristics of the Coupled Model Intercomparison Project Phase 5 (CMIP5)
513 models used in this study.

Model Name	Institution, Country	Latitudinal Grid Spacing (degree)
CanESM2	Canadian Centre for Climate Modelling and Analysis (CCCMA), Canada	2.8
CCSM4	National Center for Atmospheric Research (NCAR), USA	1.25
CSIRO-Mk3-6-0	Commonwealth Scientific and Industrial Research Organisation in collaboration with the Queensland Climate Change Centre of Excellence (CSIRO), Australia	1.9
FGOALS-g2	Institute of Atmospheric Physics, Chinese Academy of Sciences (LASG-IAP) and Tsinghua University (CESS), China	2.8
FGOALS-s2	Institute of Atmospheric Physics, Chinese Academy of Sciences (LASG-IAP), China	2.8
GFDL-ESM2G	Geophysical Fluid Dynamics Laboratory (GFDL) Earth System Model with Generalized Ocean Layer Dynamics (GOLD) component (ESM2G), USA	2.0
GFDL-ESM2M	Geophysical Fluid Dynamics Laboratory (GFDL) Earth System Model with Modular Ocean Model 4 (MOM4) component (ESM2M), USA	2.0
HadGEM2-CC	Met Office Hadley Centre (MOHC), UK; additional realizations contributed by Instituto Nacional de Pesquisas Espaciais (INPE)	1.25
HadGEM2-ES	Met Office Hadley Centre (MOHC), UK; additional realizations contributed by Instituto Nacional de Pesquisas Espaciais (INPE)	1.25
INM-CM4	Institute of Numerical Mathematics (INM) Coupled Model, Russia	1.5
IPSL-CM5A-LR	L'Institut Pierre-Simon Laplace (IPSL) Coupled Model, coupled with NEMO, low resolution, France	1.9
MIROC5	Atmosphere and Ocean Research Institute (The University of Tokyo), National Institute for Environmental Studies, and Japan Agency for Marine-Earth Science and Technology, Japan	1.4
MIROC-ESM	Atmosphere and Ocean Research Institute, National Institute for Environmental Studies, and Japan Agency for Marine-Earth Science and Technology, Japan	2.8

MIROC-ESM-CHEM	Atmosphere and Ocean Research Institute, National Institute for Environmental Studies, and Japan Agency for Marine-Earth Science and Technology, Japan	2.8
MPI-ESM-LR	Max Planck Institute for Meteorology (MPI-M), Germany	1.9
MRI-CGCM3	Meteorological Research Institute, Japan	1.1
NorESM1-M	Norwegian Climate Centre (NCC), Norway	1.9

514

515

516 Table 3. Drought index classifications for the Standardized Precipitation Index (SPI) and
517 Standardized Precipitation-Evapotranspiration Index (SPEI).

Classification	Index Value
Extremely wet (EW)	≥ 2.00
Very wet (VW)	1.50 to 1.99
Moderately wet (MW)	1.00 to 1.49
Near Normal (NN)	0.99 to -0.99
Moderate drought (MD)	-1.00 to -1.49
Severe drought (SD)	-1.50 to -1.99
Extreme drought (ED)	≤ -2.00

518

519

520 **FIGURE CAPTION LIST**

521

522 Figure 1. Study area including the four major river basins of the Han, Nakdong, Geum, and
523 Yeongsan-Sumjin rivers.

524 Figure 2. Multi-Model Ensemble (MME) and individual model simulation data means
525 compared to observation data using Dunnett multiple comparisons in the historical period for
526 each drought index and river basin.

527 Figure 3. Frequencies of severe or extreme drought using MME_part and individual weather
528 station data based on Standardized Precipitation Index 3 (SPI3) in (a) All, (b) Nakdong, (c)
529 Geum, and (d) Yeongsan-Sumjin basins. The leftmost boxplot is for the historical period
530 (1976–2005), followed by future periods (PEY2035–PEY2100) for the Representative
531 Concentration Pathways (RCP) 4.5 and 8.5 scenarios. Boxplots represent the value ranges of
532 weather stations belonging to each basin, and the open circles are area outliers.

533 Figure 4. Frequencies of severe or extreme drought using MME_part and individual weather
534 station data based on Standardized Precipitation Index 12 (SPI12) in (a) All, (b) Han, (c)
535 Nakdong, (d) Geum, and (e) Yeongsan-Sumjin basins. The leftmost boxplot is for the
536 historical period (1976–2005), followed by future periods (PEY2035–PEY2100) for the
537 Representative Concentration Pathways (RCP) 4.5 and 8.5 scenarios. Boxplots represent the
538 value ranges of weather stations belonging to each basin.

539 Figure 5. Frequencies of severe or extreme drought using MME_part and individual weather
540 station data based on Standardized Precipitation-Evapotranspiration Index 3 (SPEI3) in (a)

All, (b) Han, (c) Nakdong, (d) Geum, and (e) Yeongsan-Sumjin basins. The leftmost boxplot is for the historical period (1976–2005), followed by future periods (PEY2035–PEY2100) for the Representative Concentration Pathways (RCP) 4.5 and 8.5 scenarios. Boxplots represent the value ranges of weather stations belonging to each basin.

Figure 6. Frequencies of severe or extreme drought using MME_part and individual weather station data based on Standardized Precipitation-Evapotranspiration Index 12 (SPEI12) in (a) All, (b) Han, (c) Nakdong, (d) Geum, and (e) Yeongsan-Sumjin basins. The leftmost boxplot is for the historical period (1976–2005), followed by future periods (PEY2035–PEY2100) for the Representative Concentration Pathways (RCP) 4.5 and 8.5 scenarios. Boxplots represent the value ranges of weather stations belonging to each basin.

Figure 7. Frequencies of severe or extreme drought using individual models organizing MME_part and station-averaged data based on Standardized Precipitation Index 12 (SPI12) in (a) All, (b) Han, (c) Nakdong, (d) Geum, and (e) Yeongsan-Sumjin basins. The leftmost boxplot is for the historical period (1976–2005), followed by future periods (PEY2035–PEY2100) for the Representative Concentration Pathways (RCP) 4.5 and 8.5 scenarios. Boxplots represent the value ranges of individual models.

Figure 8. Frequencies of severe or extreme drought using individual models organizing MME_part and station-averaged data based on Standardized Precipitation-Evapotranspiration Index 3 (SPEI3) in (a) All, (b) Han, (c) Nakdong, (d) Geum, and (e) Yeongsan-Sumjin basins. The leftmost boxplot is for the historical period (1976–2005), followed by future periods (PEY2035–PEY2100) for the Representative Concentration Pathways (RCP) 4.5 and 8.5 scenarios. Boxplots represent the value ranges of individual models.

Figure 9. Average durations of severe or extreme drought using MME_part and individual weather station data based on Standardized Precipitation-Evapotranspiration Index 1 (SPEI1) in (a) All, (b) Han, (c) Nakdong, (d) Geum, and (e) Yeongsan-Sumjin basins. The leftmost boxplot is for the historical period (1976–2005), followed by future periods (PEY2035–PEY2100) for the Representative Concentration Pathways (RCP) 4.5 and 8.5 scenarios. Boxplots represent the value ranges of weather stations belonging to each basin.

Figure 10. Average durations of severe or extreme drought using individual models organizing MME_part and station-averaged data based on Standardized Precipitation-Evapotranspiration Index 1 (SPEI1) in (a) All, (b) Han, (c) Nakdong, (d) Geum, and (e) Yeongsan-Sumjin basins. The leftmost boxplot is for the historical period (1976–2005), followed by future periods (PEY2035–PEY2100) for the Representative Concentration Pathways (RCP) 4.5 and 8.5 scenarios. Boxplots represent the value ranges of individual models.

577 **FIGURES**

578

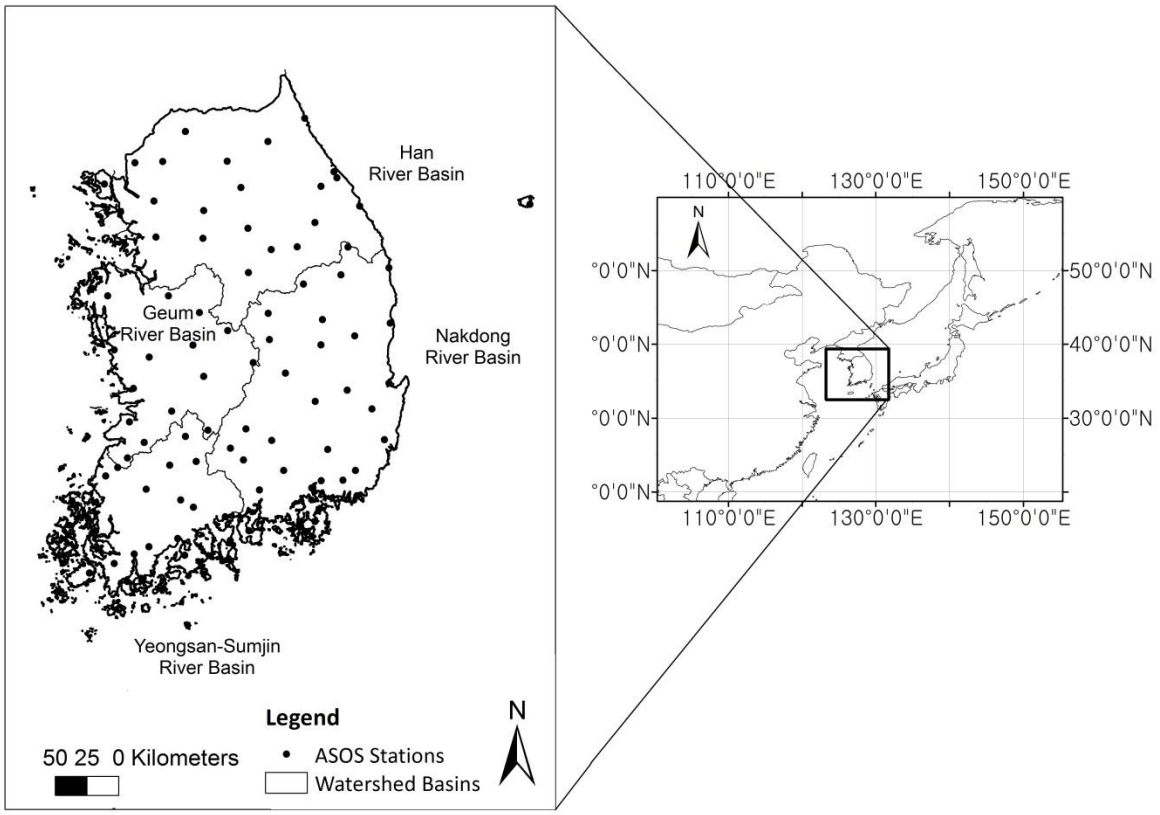

579

580 Figure 1. Study area including the four major river basins of the Han, Nakdong, Geum, and

581 Yeongsan-Sumjin rivers.

582

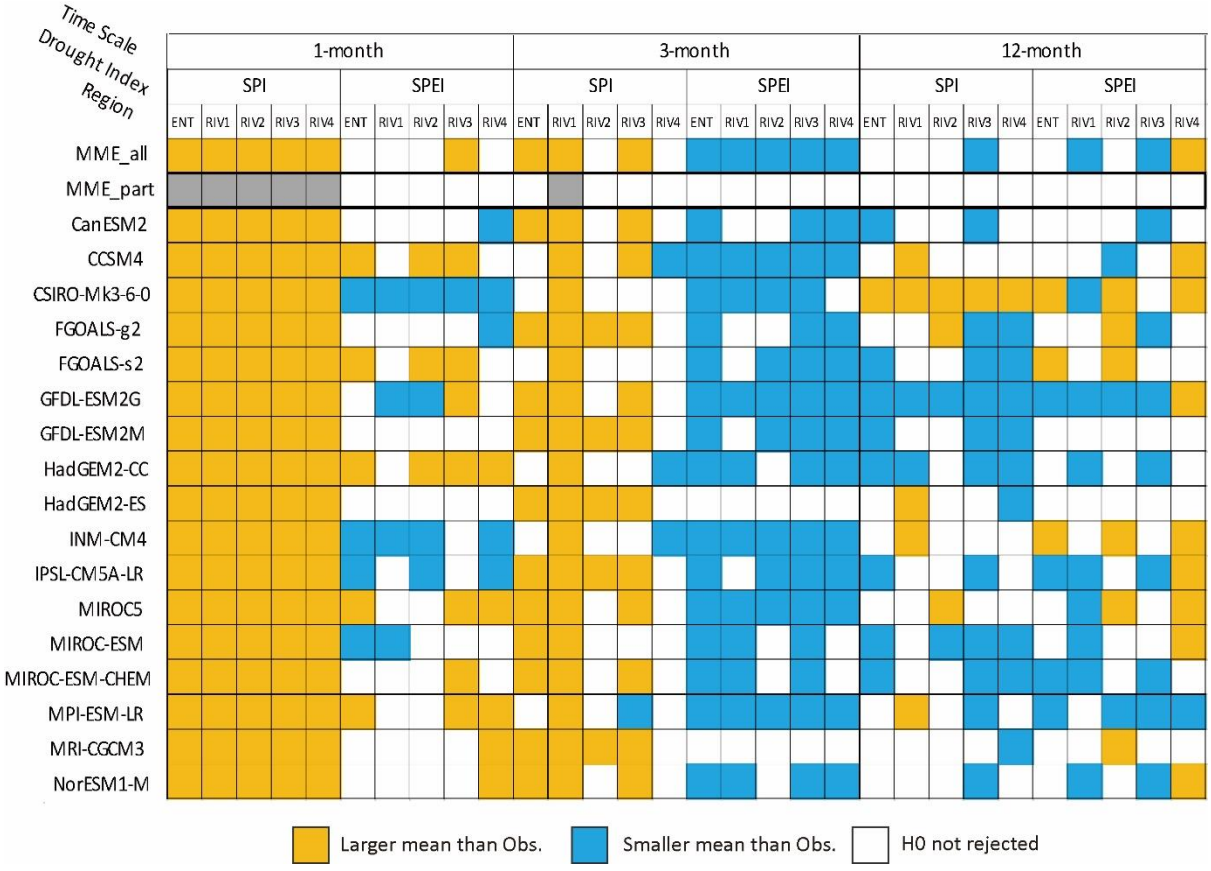

583

584 Figure 2. Multi-Model Ensemble (MME) and individual model simulation data means
585 compared to observation data using Dunnett multiple comparisons in the historical period for
586 each drought index and river basin.

587

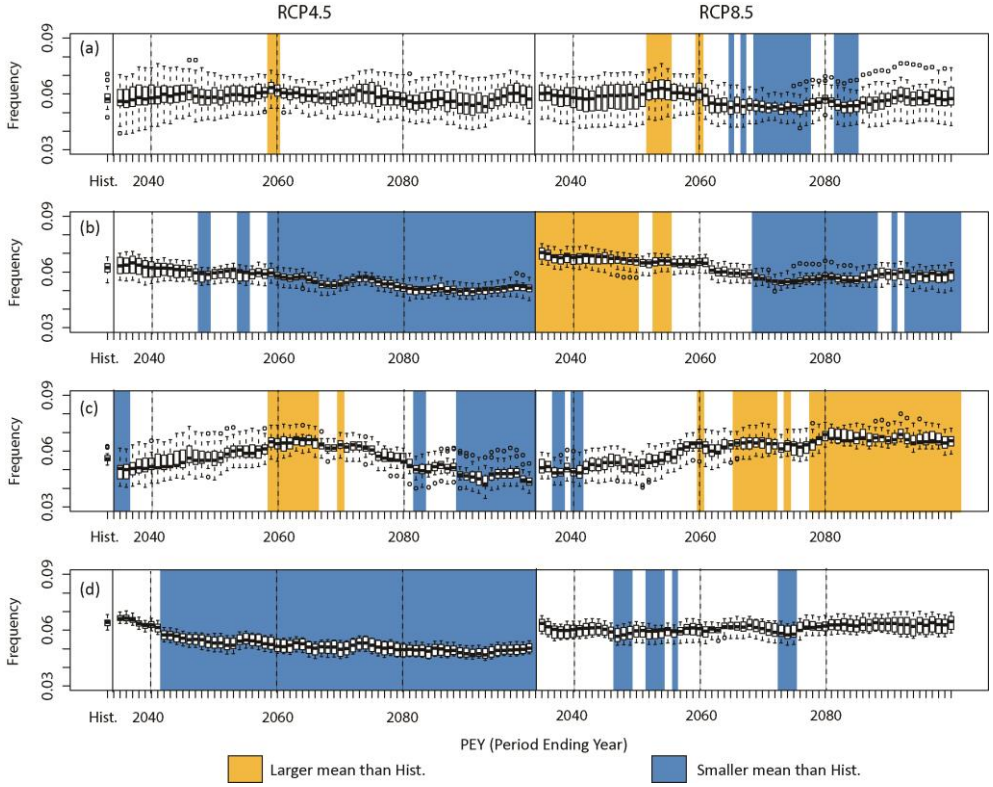

588

589 Figure 3. Frequencies of severe or extreme drought using MME_part and individual weather
590 station data based on Standardized Precipitation Index 3 (SPI3) in (a) All, (b) Nakdong, (c)
591 Geum, and (d) Yeongsan-Sumjin basins. The leftmost boxplot is for the historical period
592 (1976–2005), followed by future periods (PEY2035–PEY2100) for the Representative
593 Concentration Pathways (RCP) 4.5 and 8.5 scenarios. Boxplots represent the value ranges of
594 weather stations belonging to each basin, and the open circles are area outliers.

595

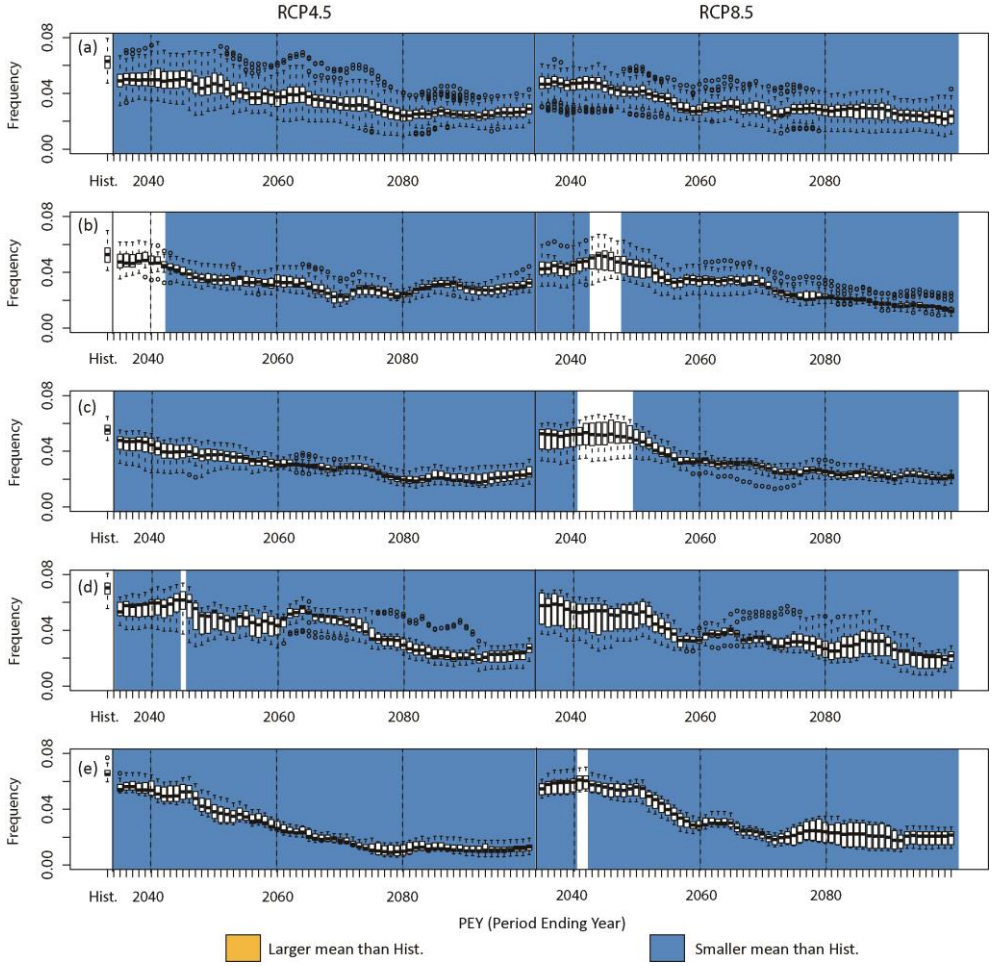

596

597 Figure 4. Frequencies of severe or extreme drought using MME_part and individual weather
598 station data based on Standardized Precipitation Index 12 (SPI12) in (a) All, (b) Han, (c)
599 Nakdong, (d) Geum, and (e) Yeongsan-Sumjin basins. The leftmost boxplot is for the
600 historical period (1976–2005), followed by future periods (PEY2035–PEY2100) for the
601 Representative Concentration Pathways (RCP) 4.5 and 8.5 scenarios. Boxplots represent the
602 value ranges of weather stations belonging to each basin.

603

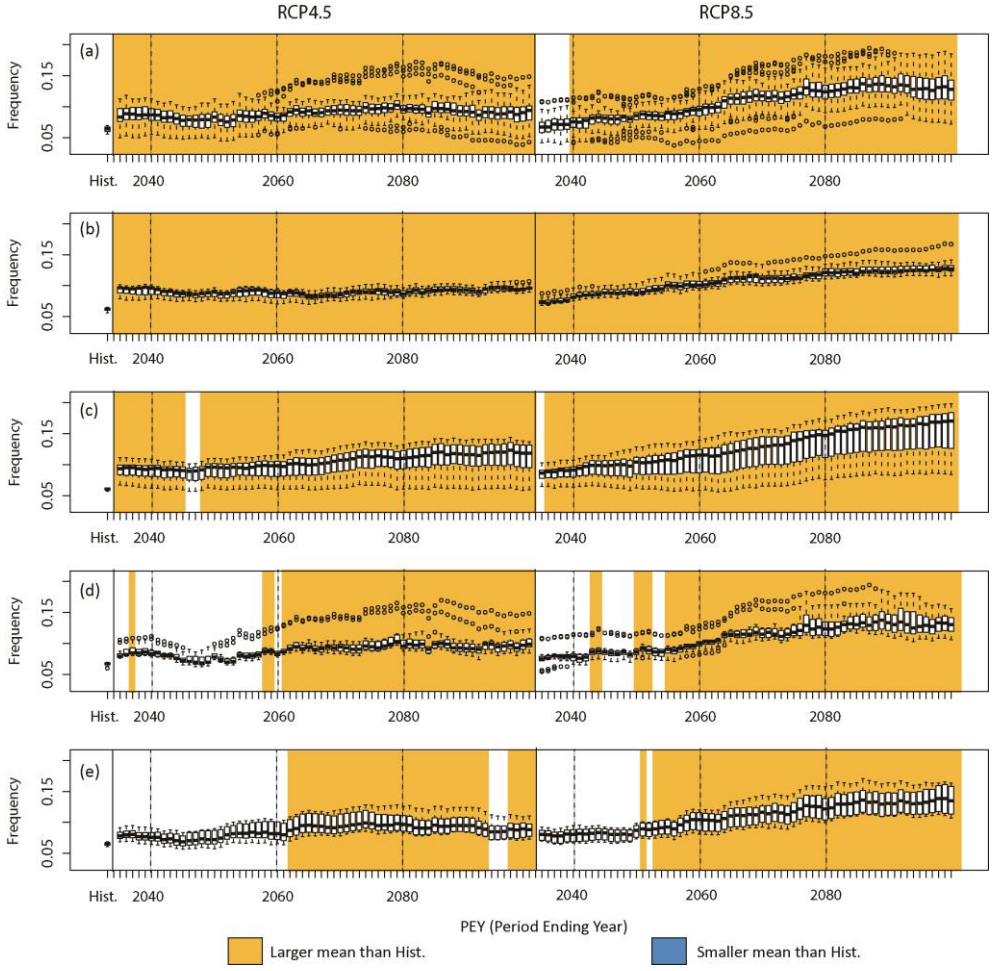

604

605 Figure 5. Frequencies of severe or extreme drought using MME_part and individual weather
606 station data based on Standardized Precipitation-Evapotranspiration Index 3 (SPEI3) in (a)
607 All, (b) Han, (c) Nakdong, (d) Geum, and (e) Yeongsan-Sumjin basins. The leftmost boxplot
608 is for the historical period (1976–2005), followed by future periods (PEY2035–PEY2100) for
609 the Representative Concentration Pathways (RCP) 4.5 and 8.5 scenarios. Boxplots represent
610 the value ranges of weather stations belonging to each basin.

611

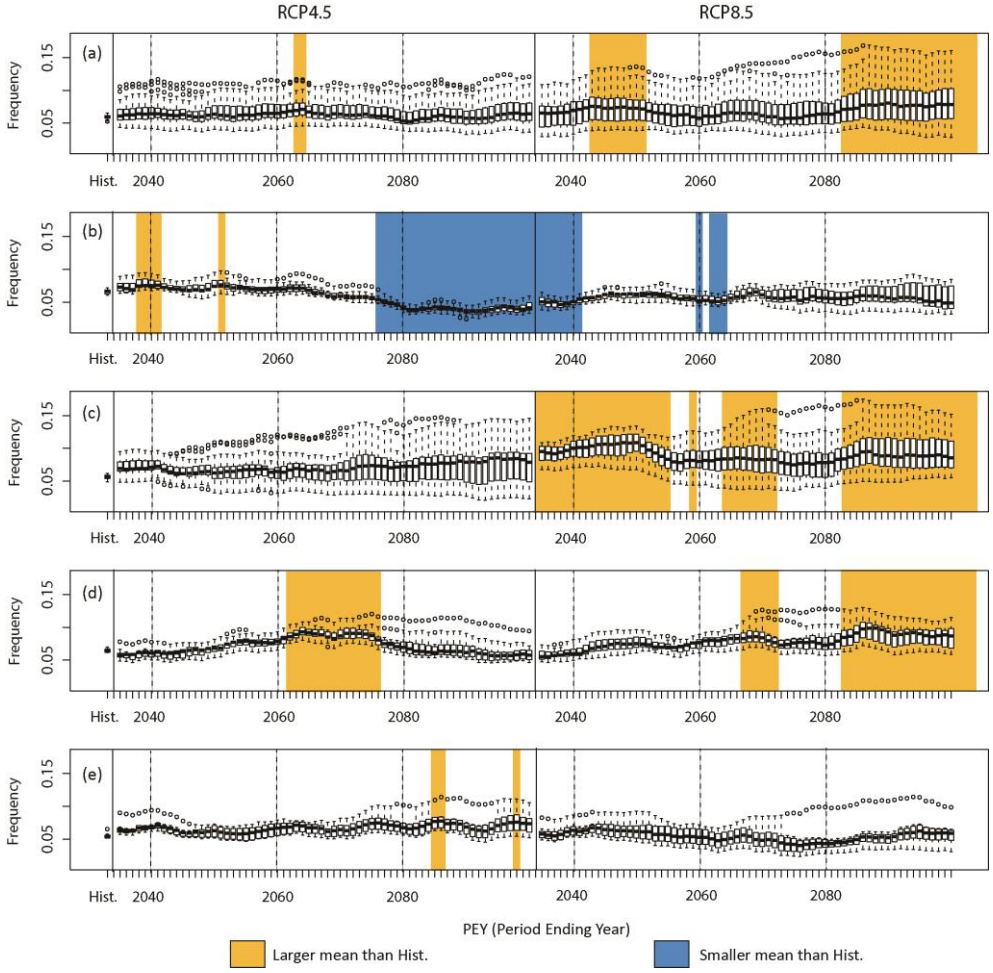

612

613 Figure 6. Frequencies of severe or extreme drought using MME_part and individual weather
614 station data based on Standardized Precipitation-Evapotranspiration Index 12 (SPEI12) in (a)
615 All, (b) Han, (c) Nakdong, (d) Geum, and (e) Yeongsan-Sumjin basins. The leftmost boxplot
616 is for the historical period (1976–2005), followed by future periods (PEY2035–PEY2100) for
617 the Representative Concentration Pathways (RCP) 4.5 and 8.5 scenarios. Boxplots represent
618 the value ranges of weather stations belonging to each basin.

619

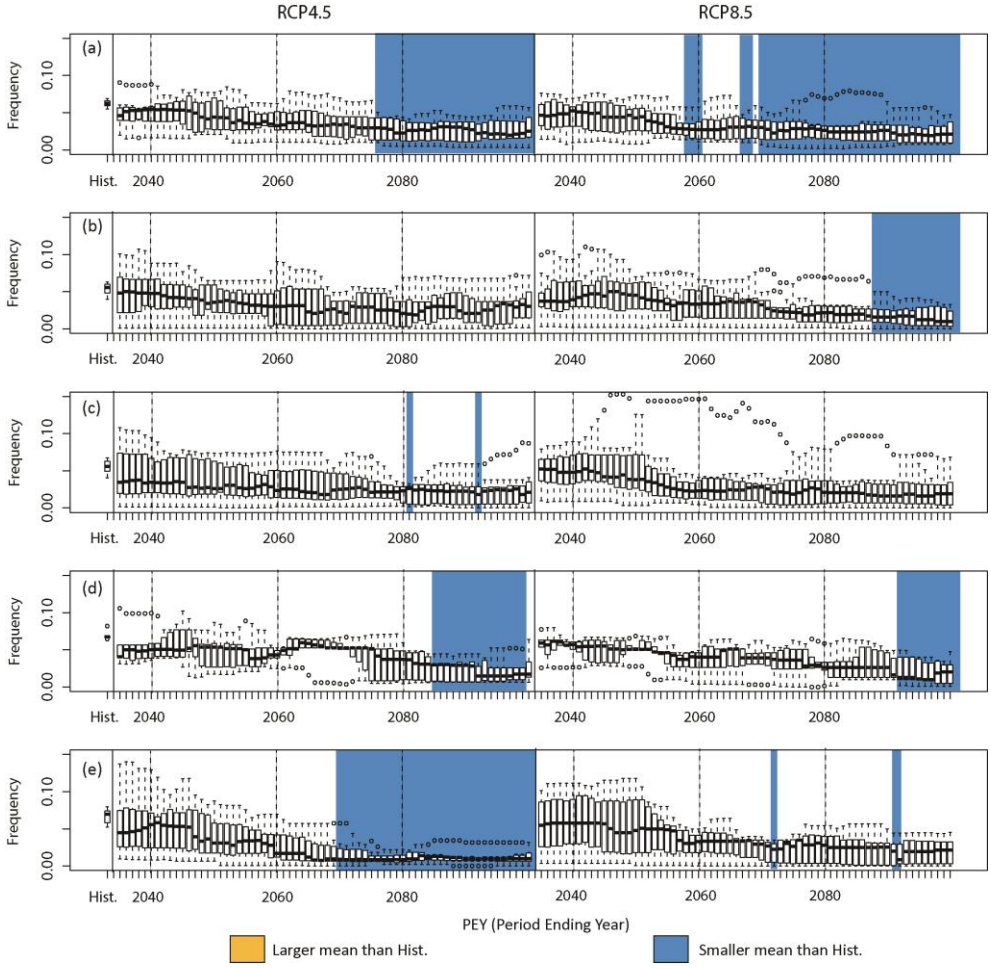

620

621 Figure 7. Frequencies of severe or extreme drought using individual models organizing
622 MME_part and station-averaged data based on Standardized Precipitation Index 12 (SPI12)
623 in (a) All, (b) Han, (c) Nakdong, (d) Geum, and (e) Yeongsan-Sumjin basins. The leftmost
624 boxplot is for the historical period (1976–2005), followed by future periods (PEY2035–
625 PEY2100) for the Representative Concentration Pathways (RCP) 4.5 and 8.5 scenarios.
626 Boxplots represent the value ranges of individual models.

627

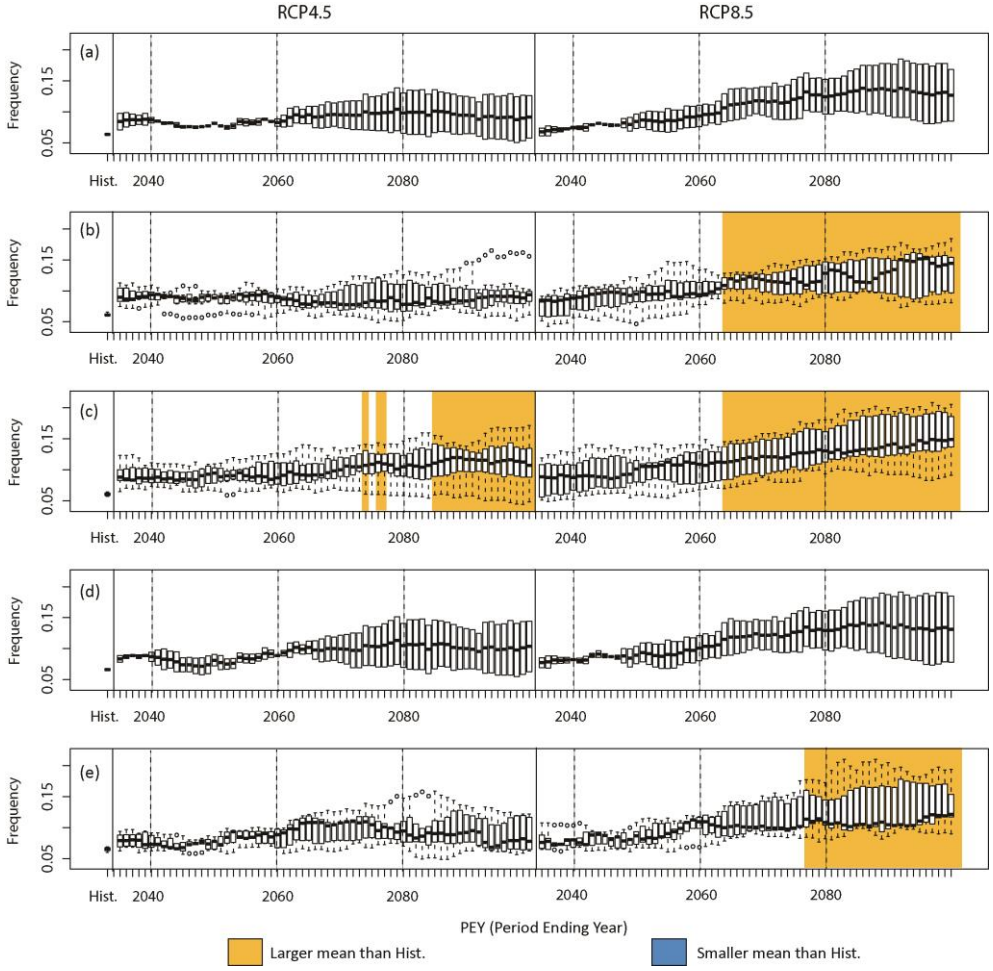

628

629 Figure 8. Frequencies of severe or extreme drought using individual models organizing
630 MME_part and station-averaged data based on Standardized Precipitation-Evapotranspiration
631 Index 3 (SPEI3) in (a) All, (b) Han, (c) Nakdong, (d) Geum, and (e) Yeongsan-Sumjin basins.
632 The leftmost boxplot is for the historical period (1976–2005), followed by future periods
633 (PEY2035–PEY2100) for the Representative Concentration Pathways (RCP) 4.5 and 8.5
634 scenarios. Boxplots represent the value ranges of individual models.

635

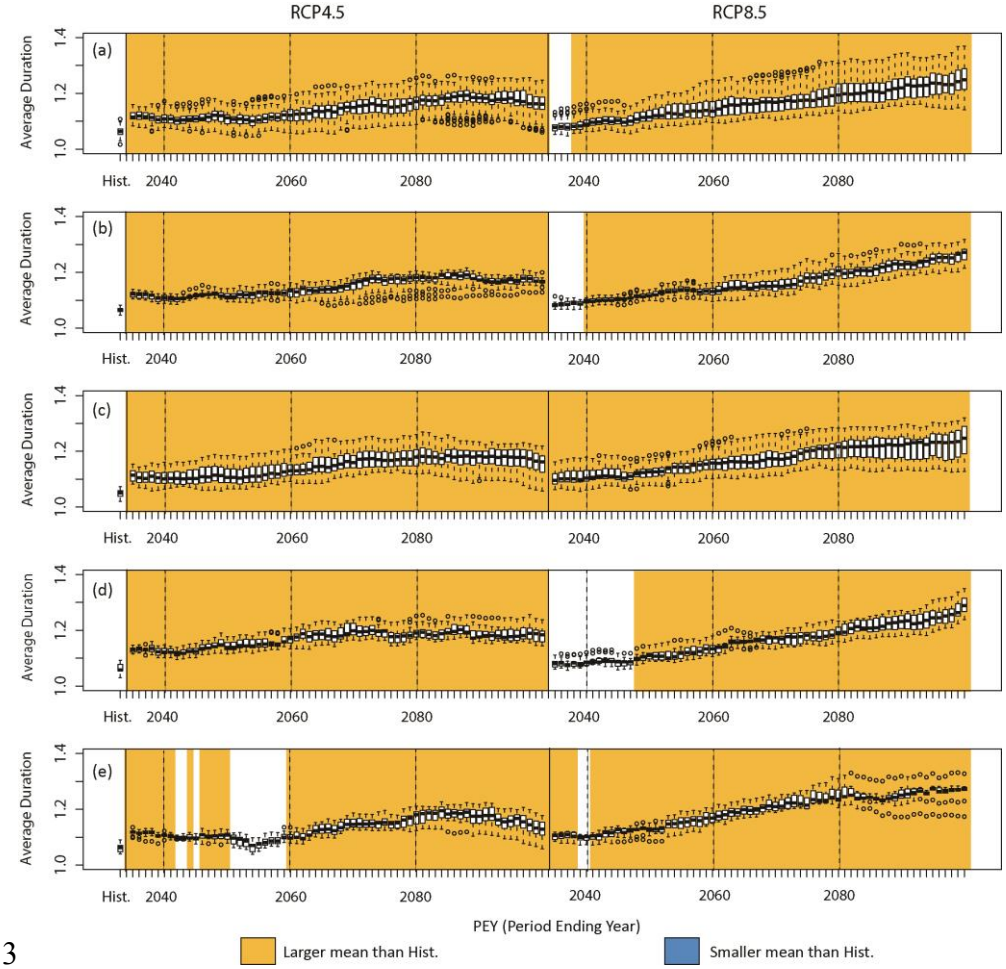

3

Figure 9. Average durations of severe or extreme drought using MME_part and individual weather station data based on Standardized Precipitation-Evapotranspiration Index 1 (SPEI1) in (a) All, (b) Han, (c) Nakdong, (d) Geum, and (e) Yeongsan-Sumjin basins. The leftmost boxplot is for the historical period (1976–2005), followed by future periods (PEY2035–PEY2100) for the Representative Concentration Pathways (RCP) 4.5 and 8.5 scenarios. Boxplots represent the value ranges of weather stations belonging to each basin.

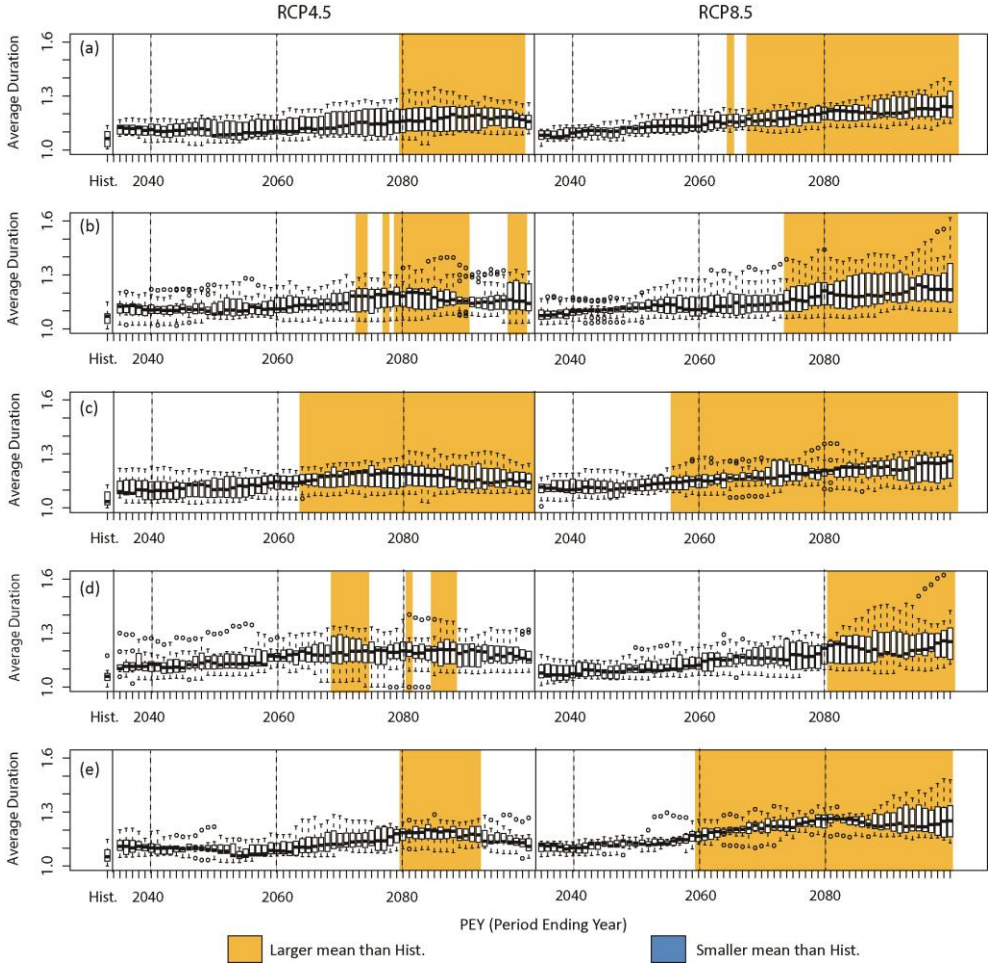

644

645 Figure 10. Average durations of severe or extreme drought using individual models
646 organizing MME_part and station-averaged data based on Standardized Precipitation-
647 Evapotranspiration Index 1 (SPEI1) in (a) All, (b) Han, (c) Nakdong, (d) Geum, and (e)
648 Yeongsan-Sumjin basins. The leftmost boxplot is for the historical period (1976–2005),
649 followed by future periods (PEY2035–PEY2100) for the Representative Concentration
650 Pathways (RCP) 4.5 and 8.5 scenarios. Boxplots represent the value ranges of individual
651 models.

652